The Journal of Immunology

TANK-Binding Kinase 1 Attenuates PTAP-Dependent Retroviral Budding through Targeting Endosomal Sorting Complex Required for Transport-I

Qi Da, Xuanming Yang, Youli Xu, Guangxia Gao, Genhong Cheng and Hong Tang

J Immunol 2011; 186:3023-3030; Prepublished online 26 January 2011;
doi: 10.4049/jimmunol.1000262
http://www.jimmunol.org/content/186/5/3023

The Journal of Immunology is published twice each month by
The American Association of Immunologists, Inc.,
1451 Rockville Pike, Suite 650, Rockville, MD 20852

Print ISSN: 0022-1767 Online ISSN: 1550-6606.

TANK-Binding Kinase 1 Attenuates PTAP-Dependent Retroviral Budding through Targeting Endosomal Sorting Complex Required for Transport-I

Qi Da,*,†,[1] Xuanming Yang,*,†,[1] Youli Xu,* Guangxia Gao,* Genhong Cheng,*,‡ and Hong Tang*

Retroviruses need to bud from producer cells to spread infection. To facilitate its budding, some virus hijacks the multivesicular body (MVB) pathway that is normally used to cargo and degrade ubiquitylated cellular proteins, through interaction between the late domain of Gag polyproteins and the components of MVB machinery. In this study, we demonstrated that TANK-binding kinase 1 (TBK1) directly interacted with VPS37C, a subunit of endosomal sorting complex required for transport-I (ESCRT-I) in the MVB pathway, without affecting the ultrastructure or general function of MVB. Interestingly, overexpression of TBK1 attenuated, whereas short hairpin RNA interference of TBK1 enhanced HIV-1 pseudovirus release from Vero cells in type I IFN (IFN-I)-independent manner. Down-regulation of TBK1 by short hairpin RNA in TZM-bl cells also enhanced live HIV-1 NL4-3 or JR-CSF virus budding without involvement of IFN-I induction. Furthermore, infection of TBK1-deficient mouse embryonic fibroblast cells with a chimeric murine leukemia virus/p6, whose PPPY motif was replaced by PTAP motif of HIV-1, showed that lack of TBK1 significantly enhanced PTAP-dependent, but not PPPY-dependent retrovirus budding. Finally, phosphorylation of VPS37C by TBK1 might regulate the viral budding efficiency, because overexpression of the kinase-inactive mutant of TBK1 (TBK1-K38A) in Vero cells accelerated HIV-1 pseudovirus budding. Therefore, through tethering to VPS37C of the ESCRT-I complex, TBK1 controlled the speed of PTAP-dependent retroviral budding through phosphorylation of VPS37C, which would serve as a novel mechanism of host cell defense independent of IFN-I signaling. ***The Journal of Immunology*****, 2011, 186: 3023–3030.**

Human endosomal sorting complex required for transport (ESCRT)-I is involved in sorting of membrane receptors into multivesicular body (MVB) pathway (1, 2). ESCRT-I is also hijacked by many enveloped viruses, including HIV-1, to promote the escape of nascent progeny virions from the infected cells. Retroviral Gag polyprotein is the only viral protein that is both necessary and sufficient to drive assembly, budding, and release of virus-like particles (3–5). In the last step of retroviral release, membrane fission event is mediated by the late budding domain (L-domain) of Gag protein, which directly or indirectly interacts with proteins of the class E vacuolar protein-sorting (VPS) pathway (4, 6). The class E VPS proteins are organized into four complexes, namely ESCRT-0, -I, -II, and -III (1, 2). TSG101, VPS28, VPS37C, and MVB12A/B form a hetero-tetramer in 1:1:1:1 stoichiometry of the human ESCRT-I complex, each of which has been identified in mediating HIV-1 release (4, 7–10). The PTAP motif of HIV-1 L-domain directly interacts with TSG101 (6), and recent studies also show that VPS37C is required for PTAP-specific HIV budding (7). Other motifs presented in enveloped viruses include PPXY, LYPXL, and FPIV motifs, which contact MVB pathway directly through interaction with AIP1/ALIX, or indirectly via interaction with HECT ubiquitin E3 ligase that connects Gag with other VPS components in ESCRT-I or ESCRT-III complexes (11, 12).

The innate immune response is a highly conserved line of defense against microbial pathogens, including viruses. Upon RNA virus infection, pattern recognition receptors including TLRs and NOD-like receptors recruit different adaptor proteins to form a scaffold, upon which serine-threonine kinase TANK-binding kinase 1 (TBK1) or the inducible IκB kinase (IKK-i/IκB kinase ε) phosphorylates IFN regulatory factor (IRF)3 (13). Phosphorylated IRF3 then dimerizes and translocates into the nucleus to activate the expression of IFN-β (14). STAT1 and STAT2 are then phsophorylated (14) once secreted IFN-β binds and activates the type I IFN receptor in an autocrine and paracine manner. Activated STAT1 and STAT2, associated with IRF9, form a transcription factor complex, IFN-stimulated gene factor 3, to initiate transcription of hundreds of effector genes, including IFN-α and IFN-β (15). TBK1–IκB kinase ε activation therefore plays a central role in IFN-β response to virus infection, in which lysine at position 38 (16) and serine at position 172 (17) are essential for TBK1 kinase activity. Although speculated as an autophosphory-

*Key Laboratory of Infection and Immunity, Chinese Academy of Sciences, Institute of Biophysics, Beijing, China; †Graduate University of Chinese Academy of Sciences, Shijingshan District, Beijing, China; and ‡Department of Microbiology, Immunology, and Molecular Genetics, University of California, Los Angeles, Los Angeles, CA 90095

[1]Q.D. and X.Y. contributed equally to this work.

Received for publication January 28, 2010. Accepted for publication December 21, 2010.

This work was supported in part by National Natural Science Foundation of China Grant 30728006 (to G.C.), a Chinese Academy of Sciences grant (KSCX1-YW-10), and Ministry of Science and Technology of People's Republic of China Grants 2006CB910901, 2006CB504205, 2007DFC30190, 2008ZX10001-002, and 2009CB522506 (to H.T.).

Address correspondence and reprint requests to Dr. Hong Tang, Key Laboratory of Infection and Immunity, Chinese Academy of Sciences, 15 Datun Road, Chaoyang District, Beijing, China 100101. E-mail address: tanghong@moon.ibp.ac.cn

The online version of this article contains supplemental material.

Abbreviations used in this article: EGF, epidermal growth factor; EGFR, EGF receptor; ESCRT, endosomal sorting complex required for transport; IKK, IκB kinase; IKK-i, inducible IκB kinase; IRF, IFN regulatory factor; MEF, mouse embryonic fibroblast; MLV, murine leukemia virus; MVB, multivesicular body; SeV, Sendai virus; shRNA, short hairpin RNA; TBK1, TANK-binding kinase 1; TEM, transmission electron microscopy; VPS, vacuolar protein-sorting; VSV, vesicular stomatitis virus; wt, wild-type.

lation site (18), a recent study shows that phosphorylation of Ser^{172} in TBK1 is mediated by an unknown protein kinase in LPS-stimulated macrophages (19). Surprising enough, besides its role in IFN-I induction, studies also reveal that, through limiting the expression of the water channel aquaporin-1 (20, 21), TBK1 is required to control cytosolic bacteria replication by maintaining the integrity of *Salmonella*-containing vacuoles. When *Salmonella* escape from *Salmonella*-containing vacuoles, TBK1 is recruited by NDP52 to restrict the proliferation of ubiquitin-coated bacteria (22).

In the search for potential regulators of TBK1, we identified that human VPS37C interacted with the C-terminal domain of TBK1 in a yeast two-hybrid screen. Further analysis showed that TBK1 might be an auxiliary component of ESCRT-I complex because it physically contacted VPS37C and was copurified with ESCRT-I complex. Functional studies revealed that TBK1 expression level was reversely correlated with the PTAP-dependent budding efficiencies of HIV-1 pseudovirus in Vero cells and murine leukemia virus (MLV)/p6 chimeric virus budding in TBK1-deficient ($Tbk1^{-/-}$) mouse embryonic fibroblast (MEF) cells. Downregulation of TBK1 by short hairpin RNA (shRNA) also enhanced the budding of both CXCR4-tropic (NL4-3) and CCR5-tropic (JR-CSF) HIV-1 viruses. IFN-I signaling was not involved in these cases, because no IFN-I production was evoked by viral infections in these cells. Further studies revealed that TBK1 negatively regulated PTAP-dependent viral budding probably through phosphorylating VPS37C. These results therefore assign a new role to TBK1 in the control of PTAP-dependent HIV-1 budding, besides its canonical role in IFN-I signaling pathway.

Materials and Methods

Abs and reagents

Polyclonal Abs from Santa Cruz Biotechnology were against epidermal growth factor receptor (EGFR) (1005), hemagglutinin (Y-11), IRF3 (FL-425), VPS28 (FL-221), and GST (Z-5). The following polyclonal Abs were against TBK1 (Cell Signaling Technology), phospho-Stat1 (Tyr^{701}; Cell Signaling Technology), GFP (Abcam), CA (Ab recognizes CA protein of molony murine leukemia virus, a gift of A. Rein, National Cancer Institute), IKK-i (a gift of B. Shu, Wuhan University), and EIAV (horse polyclonal antisera to equine infectious anemia virus, a gift of J. Zhou, Harbin Veterinary Research Institute, Chinese Academy of Agricultural Sciences). mAbs against Myc epitope (9E10), TSG101 (C-2), and Ub (P4D1) were purchased from Santa Cruz Biotechnology or from Sigma-Aldrich (β-actin [AC-15] and FLAG [M2]). HRP-conjugated goat anti-mouse/rabbit Abs (Jackson ImmunoResearch Laboratories, West Grove, PA) and HRP-conjugated goat anti-horse secondary Abs (Proteintech Group, Chicago, IL) were used for secondary Abs. γ-[^{32}P]ATP was purchased from Furui Bio (Beijing, China). Recombinant TBK1 was purchased from Invitrogen (Carlsbad, CA). TNT T7/SP6 Coupled Reticulocyte Lysate System was purchased from Promega (Madison, WI). Complete protease inhibitor mixture tablets were purchased from Roche.

Cells and viruses

HEK293T, Vero, TZM-bl, Rat2, and MEF ($Tbk1^{-/-}$, $Ikk\text{-}i^{-/-}$, and wild-type [*wt*] control) cells were routinely maintained in DMEM, and A549 cells in RPMI 1640 (HyClone). All media were supplemented with 10% FBS (PAA, Pasching, Austria), 100 U/ml penicillin, and 100 μg/ml streptomycin (HyClone). MLV and MLV/p6 viruses were produced by transfecting the plasmid pNCS or pNCS/P6-PY (a gift of P. Bieniasz, Aaron Diamond AIDS Research Center) into 293T cells, and packaged viruses were further purified, as previously described (23). HIV-1 NL4-3 and JR-CSF viruses were packaged by transfection of 293T cells with plasmids pNL4-3 (24) and pYK-JR-CSF (25), respectively (a gift of L. Zhang, Institute of Biophysics, Beijing, China).

Generation of TBK1 knockdown stable cell lines

To establish cell lines stably expressing shRNA specific for TBK1, A549 or TZM-bl cells were seeded in a 12-well plate overnight and transfected with 1.6 μg pSuper.puro-TBK1 (designated as A549/shTBK1 and TZM-bl/shTBK1) or pSuper.puro-scrambled (designated as A549/shScr and TZM-bl/shScr) using Lipofectamine 2000 (Invitrogen). After 36 h, the cells were trypsinized, 20-fold diluted, and cultured in the presence of 1 μg/ml puromycin (Sigma-Aldrich). The selected monoclonal cell lines were verified by immunoblotting. The shRNA targeting sequence for human TBK1 was 5′-GACAGAAGTTGTGATCACA-3′.

Immunoprecipitation

Transient expression of various expression constructs of VPS37C and TBK1 where indicated was routinely carried out in 5×10^5 293T cells with the standard calcium–phosphate transfection method for 36 h. Cells were then lysed with 200 μl immunoprecipitation buffer (50 mM Tris-HCl [pH 7.5], 150 mM NaCl, 0.5% Nonidet P-40, 1 mM EDTA, 1 mM PMSF, and 1× protease inhibitor mixture [Roche]), and 2 μg indicated Abs were used for immunoprecipitation. Protein complexes were then separated by SDS-PAGE and immunoblotted with indicated Abs.

Immunoblotting

Immunoprecipitated proteins, cell lysates, or supernatants were separated by 10 or 12% SDS-PAGE. Proteins were then transferred to Immobilon-P membranes (Millipore, MA), and membranes were blotted with TBS plus 0.5% Tween 20 (TBST [pH 7.4]) containing 5% nonfat milk at room temperature for 1 h. The blots were probed with indicated primary Abs, followed by an appropriate HRP-conjugated secondary Ab for chemiluminescence analysis (ECL; Pierce).

HIV-1 budding assay

Plasmids (0.8 μg pHEF-VSVG and 1.6 μg pNL4-3.Luc.R^-E^-) were transfected into 5×10^5 Vero cells to package HIV-1 pseudovirus, as previously described (26). To study the effect of TBK1 on HIV-1 pseudovirus release, 0.8 μg pECFP-TBK1, pECFP-TBK1(K38A), or pSuper.puro-TBK1, where indicated, was cotransfected. At 36 h post-transfection, 200 μl supernatants were collected to infect 293T cells (1×10^5) in triplicates for 24 h. Budding efficiency was determined by the ratio of the luciferase activities in infected 293T cells to those in Vero cells. Relative budding efficiencies were derived after normalized to the sham vector controls. To assay HIV-1 budding, TZM-bl/shTBK1 and TZM-bl/shScr control cells (2×10^5) were infected with HIV-1 isolates NL4-3 or JR-CSF (20 μl) for 2 h in the presence of 4 μg/ml polybrene (Sigma-Aldrich). Cells were then switched to the complete DMEM for additional 34 h. The supernatants (200 μl) were collected to infect TZM-bl cells (1×10^5) in triplicates for 24 h. The HIV-1 LTR-driven luciferase activities in TZM-bl and TZM-bl/shTBK1 cells were measured separately. The budding efficiencies were represented as the ratio of the luciferase activity in TZM-bl cells to that in TZM-bl/shTBK1 or TZM-bl/shScr cells.

MLV budding assay

Wt and $Tbk1^{-/-}$ MEFs (5×10^4) were infected with 30 μl MLV/p6 or MLV virus for 2 h in the presence of 8 μg/ml polybrene (Sigma-Aldrich). Cells were then switched to complete DMEM for the time indicated. The viruses in the supernatant were concentrated by ultracentrifugation through a 25% sucrose cushion (P40ST rotor, 100,000 × *g* at 4°C for 2 h) and lysed in 100 μl SDS-PAGE loading dye. The cells were directly lysed in the same volume of the loading dye in parallel. The amounts of Gag and CA proteins were determined by immunoblotting, and the budding efficiency at each time point was calculated as the ratio of Gag plus CA proteins in the supernatant to those in cells, as previously described (27). To independently quantify the released virions, 1 ml supernatants from *wt* or $Tbk1^{-/-}$ MEFs infected by MLV or MLV/p6 were used to infect Rat2 cells (1×10^6). The de novo synthesis of MLV DNA in Rat2 cells that represented the infectivity of the budded virus was quantified by PCR analysis, as previously described (28).

EIAV virus-like particle budding assay

Plasmids (24 μg; E. Freed, National Cancer Institute) encoding EIAV Gag whose original p9 YPDL motif had been replaced by MLV p12 PPPY (EIAV/PPPY) or HIV-1 p6 PTAP (EIAV/PTAP) motif (29) were transfected into *wt* and $Tbk1^{-/-}$ MEFs (1×10^6) by Lipofectamine 2000. Forty-eight hours later, virus-like particles secreted in the supernatants were concentrated by ultracentrifugation through a 20% sucrose cushion (P40ST rotor, 100,000 × *g* at 4°C for 1 h) and lysed in 40 μl SDS-PAGE loading dye. The cells were also lysed in equal volume of the loading dye. The amount of Gag proteins of virions was determined by immunoblotting, and the budding efficiency was represented as the ratio of Gag proteins in the supernatants to those in cells, as mentioned above.

IFN-β activation assays

Native PAGE analysis of dimerized IRF3, an indication of IFN-β gene activation, and quantitative RT-PCR analysis of *ifn-β* mRNA production were performed exactly as previously described (30).

EGFR degradation assay

Quantification of EGFR degradation was performed, as previously described, with some modifications (31). In brief, A549/shScr and A549/shTBK1 cells were serum starved in DMEM/0.1% FBS for 12 h before stimulated with 100 ng/ml recombinant human EGF for the time indicated. The amount of EGFR was then assessed by immunoblotting with anti-EGFR Ab and quantified with a densitometer (Alpha Innotech).

Column chromatography

Approximately 3×10^7 *wt* or *Tbk1*$^{-/-}$ MEFs were lysed in 1.5 ml lysis buffer (PBS, 0.1% Tween 20, 1× protease inhibitor mixture) and centrifuged (16,000 × *g*) at 4°C for 1 h to clear cell debris before applied to size exclusion chromatography (Superdex G200 10/300, flow rate 0.5 ml/min). Fractions were precipitated with trichloroacetic acid and analyzed by immunoblotting with Abs against TBK1, TSG101, and VPS28, respectively. Peak fractions containing ESCRT-I and TBK1 were further subjected to anionic chromatography (HiTrap Q HP 7/25, the salt gradient 30–1000 mM NaCl). All fractionation was performed with an Äkta Explorer (GE Healthcare, Uppsala, Sweden).

Kinase assays

HEK293T cells (5×10^5) were individually transfected with 2.5 μg pCMV-Flag-VPS37C, pCMV-Flag-TBK1, or pCMV-Flag-TBK1-K38A. Ectopically expressed proteins were immunoprecipitated separately with anti-M2 agarose beads (Sigma-Aldrich). VPS37C and TBK1 on beads were then mixed, as indicated, in 25 μl kinase assay buffer (25 mM HEPES [pH 7.4], 1 mM DTT, 50 mM KCl, 2 mM $MgCl_2$, 2 mM $MnCl_2$, 10 mM NaF, 1 mM Na_3VO_4, 25 μM ATP, and 0.2 μCi/μl γ-[^{32}P]ATP) at 25°C for 1 h. Alternatively, recombinant GST or GST-VPS37C preabsorbed on beads (5 μl, 75% slurry) were mixed with 80 ng recombinant TBK1 (Invitrogen) in 25 μl kinase assay buffer at 25°C for 1 h. Proteins were separated by SDS-PAGE, and phosphorylation of VPS37C was detected by a PhosphorImager scanner (Typhoon Trio$^+$; GE Healthcare).

Transmission electron microscopy

To visualize viral budding, *wt* or *Tbk1*$^{-/-}$ MEFs (5×10^5) were infected with MLV/p6 virus (600 μl) for 48 h. To inspect the ultrastructure of MVB, MEF cells were incubated with 100 ng/ml recombinant EGF and BSA–gold conjugates (Φ = 10 nm, OD_{520} = 8; a gift of M. Xiao, Peking University) for 2 h. Infected or EGF-stimulated cells were then fixed with 2% glutaraldehyde, embedded in Epon812, and ultrathin sectioned (EMUC6; Leica) for transmission electron microscopy (120 kV, ×5000; Philips Tecnai 20, FEI, Hillsboro, OR), as previously described (23). The number of BSA–gold-positive MVB and the size (μm^2) of MVB from 128 view fields were calculated, as previously described (32), except that IQStudio software (Media Cybernetics, Bethesda, MD) was applied for measuring the area of MVB.

Statistical analysis

The results were expressed as the mean ± SEM or mean ± SD, as indicated. Groups of data were compared by two-tailed unpaired Student's *t* test. Differences were considered to be statistically significant when $p < 0.05$.

Results

TBK1 interacts with VPS37C constitutively

We initially identified a fragment of VPS37C (aa 83–263) that could contact the C terminus of TBK1 (aa 311–729) in a yeast two-hybrid screening. Such an interaction was confirmed by coimmunoprecipitation of TBK1 and VPS37C ectopically expressed in 293T cells (Fig. 1*A*). The kinase-inactive mutant of TBK1 (K38A) could precipitate VPS37C as efficiently as wt TBK1 (Fig. 1*A*), suggesting that the kinase activity of TBK1 and/or phosphorylation of VPS37C was not required for the intermolecular association. To substantiate this notion, we performed

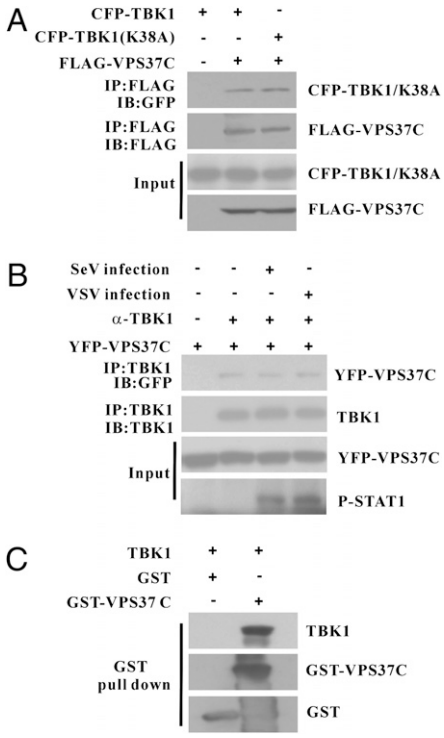

FIGURE 1. TBK1 constitutively interacts with VPS37C. *A*, Both TBK1 and its kinase-inactive mutant TBK1-K38A interacted with VPS37C. Expression vectors pECFP-TBK1 and pECFP-TBK1(K38A) were cotransfected with or without pCMV-Flag-VPS37C into 293T cells. Cell lysates were immunoprecipitated with anti-Flag Ab and immunoblotted with anti-GFP and anti-Flag Ab (*top panels*). The input of Flag-VPS37C and CFP-TBK1 was also shown (*bottom panels*). *B*, TBK1 and VPS37C remained associated after SeV and VSV infection. HEK293T cells transiently transfected with pEYFP-VPS37C plasmid were infected with SeV (multiplicity of infection = 1) or VSV (multiplicity of infection = 0.1), and the protein complexes were immunoprecipitated with anti-TBK1 Ab and immunoblotted with anti-GFP and anti-TBK1 Abs. Input of YFP-VPS37C was shown in the *bottom panel*. STAT1 phosphorylation was measured to verify the status of IFN-I induction. *C*, GST-VPS37C pulled down in vitro translated TBK1. Recombinant GST or GST-VPS37C was purified from *Escherichia coli* and mixed with in vitro translated TBK1. Proteins pulled down by glutathione–Sepharose beads were resolved by SDS-PAGE for subsequent immunoblotting with anti-GST or anti-TBK1 Ab, respectively. Data were representative of three independent experiments (*A–C*).

coimmunoprecipitation of expressed VPS37C with endogenous TBK1 in 293T cells infected with Sendai virus (SeV) or vesicular stomatitis virus (VSV). These two viruses are known to activate TBK1 kinase activity (33, 34). The results showed that TBK1 and VPS37C were in the same complex before or after viral infection (Fig. 1*B*). Constitutive association of TBK1 with VPS37C was also shown in HIV-1 NL4-3 isolate-infected TZM-bl cells (Supplemental Fig. 1). Therefore, these results indicated that TBK1 constitutively interacted with VPS37C in cells. To exclude the possibility of indirect association between overexpressed TBK1 and VPS37C, we then performed GST pull-down experiments, in which in vitro translated TBK1 could readily interact with recombinant GST-VPS37C (Fig. 1*C*). By truncational analysis, we further mapped that VPS37C used its N terminus (aa 1–155) containing a Mod(r) domain and a predicted coiled-coil domain (35) to contact the N terminus (aa 1–600) of TBK1 (Supplemental Fig. 2). Because the fragment of TBK1 (aa 311–729) interacted with VPS37C in the yeast two-hybrid assays, TBK1 thus most likely used its middle segment (aa 311–600) to contact VPS37C.

TBK1 is an auxiliary subunit of ESCRT-I

Because TBK1 interacted with VPS37C, we speculated that TBK1 might be a functional component of ESCRT-I complex. Coimmunoprecipitation experiments showed that overexpressed VPS37C could pull down both TSG101 and VPS28 of the ESCRT-I and TBK1 in the same immunocomplex (Fig. 2*A*). Furthermore, size exclusion chromatographic analysis of ESCRT-I complex (9) showed that the endogenous TBK1 coeluted with TSG101 and VPS28 in wt MEFs (the approximate complex size ~350 kDa), with TBK1 exhibiting slightly wider fraction distribution than ESCRT-I (Fig. 2*B*). Fractions 5–6 from the size exclusion (Fig. 2*B*) were further subjected to ion exchange chromatography, and TBK1 and TSG101/VPS28 still coeluted even at rather high salt concentration (400 mM; Fig. 2*C*). These results indicated that TBK1 associated with ESCRT-I rather tightly.

Although biochemically coeluted with the ESCRT-I complex, TBK1 seemed dispensable for the overall structure or general function of MVB. First, lack of TBK1 did not affect the ESCRT-I composition and stability because TSG101 and VPS28 in *Tbk1*$^{-/-}$ cells had the same fraction distribution pattern as that in wt MEFs (Fig. 2*B*). Examination of the fine structure of MVB, defined as vacuoles (with ≥1 internal vesicles) that contain internalized BSA–gold conjugates under transmission electron microscopy (TEM) (32), revealed similar ultrastructure (Fig. 3*A*) and size (Fig. 3*B*) in wt and *Tbk1*$^{-/-}$ cells, with the number of MVBs/μm^2 cytosolic area slightly more in *Tbk1*$^{-/-}$ MEFs (Fig. 3*C*). Increased number of MVB vesicles in *Tbk1*$^{-/-}$ cells would imply that TBK1 might affect protein traffic efficiency in general. Surprisingly enough, when we assessed EGF-induced EGFR degradation as a functional readout of MVB (36), shRNA knockdown of TBK1 did not affect EGFR degradation in A549 cells (Fig. 3*D*). Taken together, TBK1 might be an auxiliary component of ESCRT-I that modulates a specific facet of MVB function.

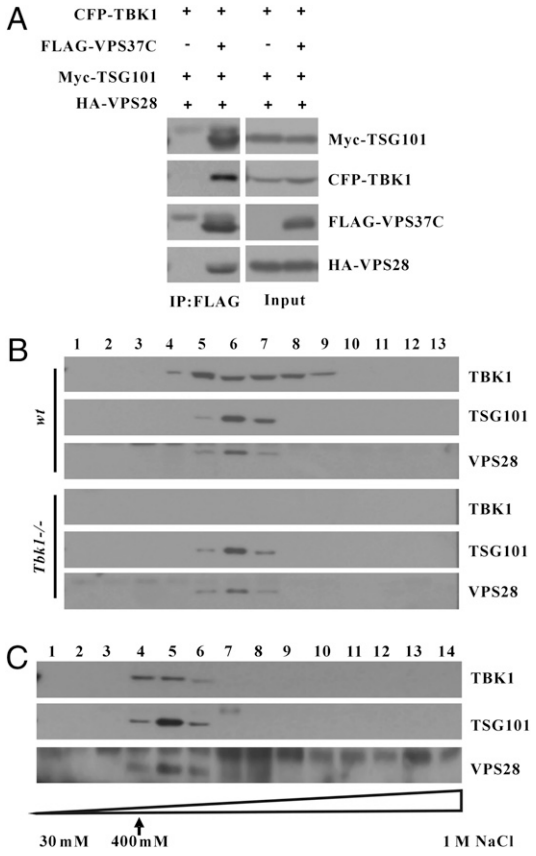

FIGURE 2. TBK1 associates with ESCRT-I complex. *A*, VPS37C coimmunoprecipitated with TBK1, TSG101, and VPS28. Equal amount of pCMV-Myc-TSG101, pCMV-HA-VPS28, and pECFP-TBK1 was cotransfected with or without pCMV-Flag-VPS37C into 293T cells. Cell lysates were immunoprecipitated with anti-FLAG Ab and immunoblotted with Abs against different fusion tags (*left panels*). Input was shown for each overexpressed protein (*right panels*). *B*, Endogenous TBK1 coeluted with the ESCRT-I complex. Cell lysates of *wt* and *Tbk1*$^{-/-}$ MEFs were fractionated through Superdex G200 size-exclusion chromatography. Indicated fractions were TCA precipitated and analyzed by immunoblotting with Abs against TBK1, TSG101, and VPS28, respectively. *C*, TBK1 tightly associated with ESCRT-I. The fractions 5–6 from *B* were subjected to ion exchange chromatography (NaCl gradient 30–1000 mM), and resultant fractions were analyzed by immunoblotting, as in *B*. Data were representative of three independent experiments (*A*–*C*).

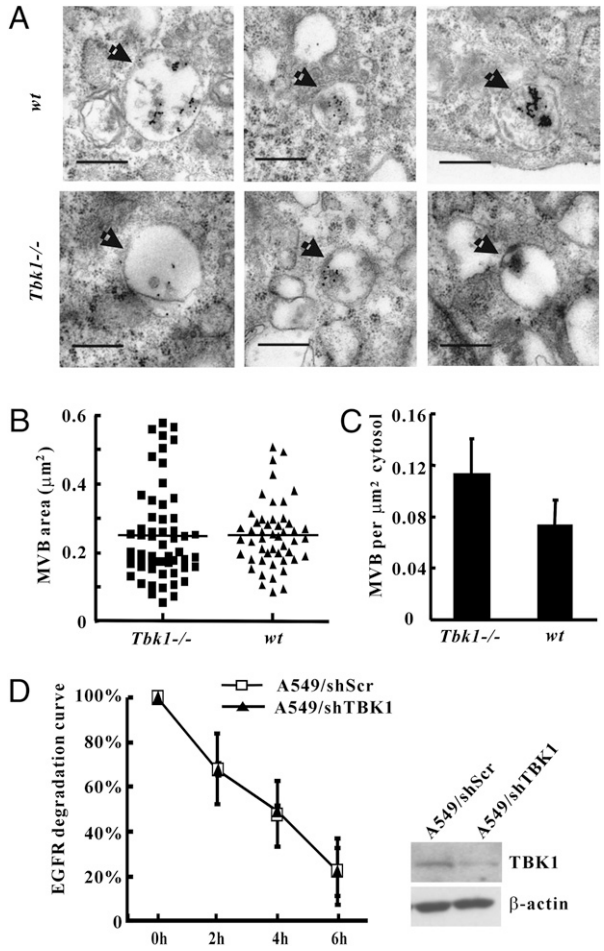

FIGURE 3. TBK1 does not affect the structure and receptor degradation function of MVB. *A*, MVBs in *wt* and *Tbk1*$^{-/-}$ MEFs had similar ultrastructure. *Wt* and *Tbk1*$^{-/-}$ MEFs were incubated with 10 nm BSA–gold conjugates at 37°C for 2 h. Cells were fixed for TEM analysis. Arrows indicated BSA–gold containing MVBs. Scale bars, 200 nm. *B*, MVBs in *wt* and *Tbk1*$^{-/-}$ MEFs had similar size. The area of BSA–gold containing vacuoles (n = 57 [*Tbk1*$^{-/-}$] and n = 49 [*wt*]) under TEM was averaged. No significant variation was scored by Student's unpaired two-tailed t test (p = 0.9468). *C*, *Tbk1*$^{-/-}$ MEFs had more MVBs than *wt* cells. The number of MVBs/μm^2 in the cytoplasm of each ultrathin section was counted and averaged from 30 independent ultrathin sections (mean ± SD). *D*, Knockdown of TBK1 did not affect EGFR degradation. TBK1 expression in A549 was stably downregulated by shRNA (knockdown efficiency shown in the *insert* by anti-TBK1 Ab blotting). Cells were then stimulated with 100 ng/ml recombinant human EGF for the time indicated. EGFR levels of TBK1 knockdown or mock cells were analyzed by immunoblotting. Data were average of at least three independent experiments (mean ± SD).

TBK1 controls PTAP-dependent viral budding independent of IFN-I induction

As VPS37C and other ESCRT-I complex components were required for HIV-1 budding (7, 10, 37), we then examined whether association of TBK1 with VPS37C might be involved in the regulation of HIV-1 budding. Transient downregulation of endogenous TBK1 by shRNA in Vero cells caused more efficient budding of HIV-1 pseudovirus than that by overexpressed TBK1 (Fig. 4*A*). We chose to use Vero cells because Vero cells were intrinsically defective in producing IFN-I (38); therefore, antiviral effects of IFN-I were not involved in the regulation of viral budding efficiency after TBK1 expression level was altered. Because HIV-1 pseudovirus packaging represents only a single-round budding process, an authentic viral infection is desired to determine whether HIV-1 budding is indeed controlled by TBK1 independent of its ability of IFN-I activation. TZM-bl cells are derived from CXCR4-positive HeLa cells by stably expressing CD4 and CCR5 (39) and a HIV-1 LTR-driven cassette of luciferase and β-galactosidase genes (40). We further engineered TZM-bl cells by shRNA stable knockdown of TBK1 gene (Fig. 4*B*). When infected with HIV-1 NL4-3 [CXCR4 tropic (41)] or JR-CSF [CCR5 tropic (42)] virus for 36 h, TZM-bl/shTBK1 cells released more viral particles than the TZM-bl/shScr control cells (Fig. 4*B*). Infection of TZM-bl cells with HIV-1 did not activate IFN-I signaling as STAT1 remained unphosphorylated in response to NL4-3 infection (Fig. 4*C*). Therefore, activation of IFN-I production is dispensable for TBK1 to control HIV-1 budding velocity.

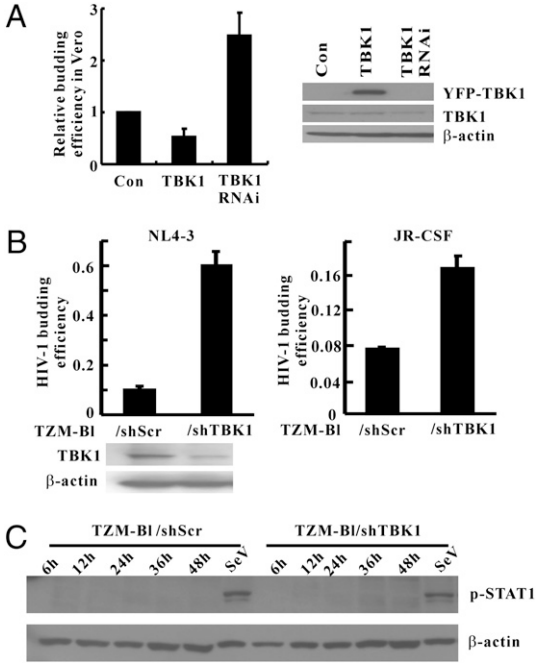

FIGURE 4. TBK1 inhibits HIV-1 budding independent of IFN-I. *A*, The level of TBK1 affected budding efficiency of HIV-1 pseudovirus. HIV-1 pseudovirus packaging plasmids (pHEF-VSVG and pNL4-3.Luc.R$^-$E$^-$) were cotransfected with pECFP-TBK1 or pSuper.puro-TBK1 plasmid into Vero cells. HIV-1 pseudoviruses in supernatants were collected 36 h post-transfection, and the amount of virus particles was quantified by their luciferase activities postinfection of 293T cells. Budding efficiencies were calculated as the ratio of the luciferase activities in 293T cells to that in the packaging Vero cells. Relative budding efficiency was normalized to budding efficiency in control cells in each sample. The expression levels of TBK1 and β-actin were shown. Data were average of at least three independent experiments after normalization (mean ± SEM). *B*, Downregulation of TBK1 could enhance HIV-1 budding efficiency. TBK1 gene expression was stably knockdown in TZM-bl to yield TZM-b/shTBK1 (scrambled shRNA control TZM-bl/shScr). Cells were infected with HIV-1 NL4-3 and JR-CSF isolates, and released virus particles were collected to infect TZM-bl for luciferase activity measurement. Budding efficiency was represented as the ratio of the luciferase activity in TZM-bl cell over that in TZM-bl/shTBK1 or TZM-bl/shScr cells. The expression levels of TBK1 and β-actin in TZM-bl/shTBK1 and TZM-bl/shScr cells were shown. Data were presented as the average of three independent experiments (mean ± SD). *C*, HIV-1 infection did not induce IFN-I in TZM-bl cells. TZM-bl/shTBK1 and TZM-bl/shScr cells (1×10^5) were infected with 200 μl HIV-1 NL4-3 stock for the time indicated, and cell lysates were prepared for immunoblotting of phosphor-STAT1 and β-actin. Data were representative of two independent experiments.

We next went on to address whether TBK1 controls retroviral budding in a PTAP-dependent mode. We first used a chimeric virus MLV/p6, which is engineered by replacing the original PPPY motif of MLV p12 with HIV-1 p6 PTAP motif (23) and therefore exhibits PTAP-dependent budding that is regulated by VPS37C (7). MLV/p6 infection of MEFs within the time frame of 48 h did not induce IFN-I induction, as evidenced by null production of IFN-β (Supplemental Fig. 3*A*), IRF3 dimerization (Supplemental Fig. 3*B*), or STAT1 phosphorylation (Supplemental Fig. 3*C*). MLV/p6 virus released more efficiently from *Tbk1*$^{-/-}$ than from wt cells (Fig. 5*A*, 5*B*), as measured by the ratio of the sum of Gag and CA

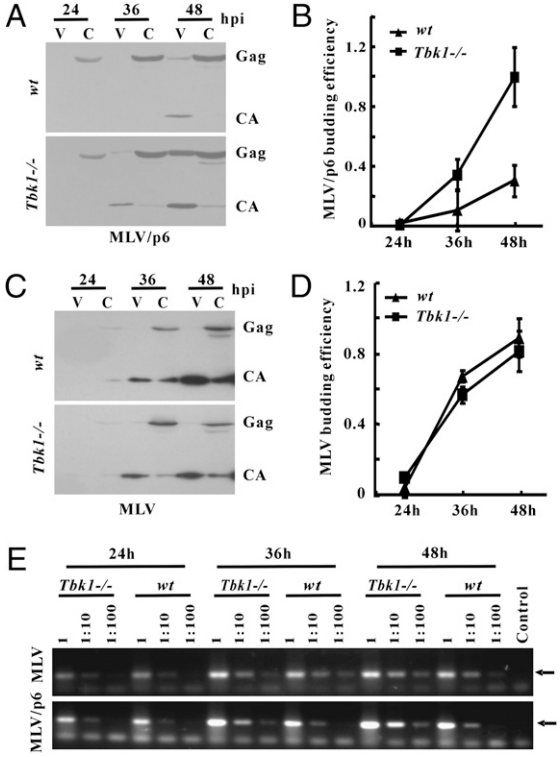

FIGURE 5. TBK1 inhibits PTAP-dependent retrovirus budding independent of IFN-I. *A–D*, Lack of TBK1 enhanced PTAP-dependent virus budding. *Wt* (▲) and *Tbk1*$^{-/-}$ (■) MEFs were infected with MLV/p6 (*A*) or MLV (*C*) for the time indicated. Virions in supernatants (V) and in cells (C) were collected and quantified by immunoblotting with anti-CA Ab (*B* and *D*, respectively). The budding efficiency was defined as the ratio of the amounts of Gag and CA proteins in V to that in C. All data were the average of at least three independent experiments (mean ± SD). *E*, Lack of TBK1 increased budding of infectious MLV/p6. *Wt* and *Tbk1*$^{-/-}$ MEFs were infected with MLV or MLV/p6, and supernatants were collected at the time indicated to infect Rat2 cells. Viral DNA was then extracted for PCR analyses with minus strand strong stop DNA primers specifically amplified the minus strand strong stop DNA of MLV. Arrows indicated the PCR products. Data shown were representative of three independent experiments.

proteins in the supernatants to that within cells. MLV buds via a PPPY-dependent manner (23) independent of VPS37C (7). As expected, MLV exhibited a similar budding kinetics in wt to that in *Tbk1*$^{-/-}$ MEFs (Fig. 5*C*, 5*D*). To independently measure the release speed, supernatants containing MLV or MLV/p6 virions from abovementioned experiments were collected to infect Rat2 cells. Assessment of de novo viral DNA synthesis in Rat2 cells by PCR analysis (28) confirmed that *Tbk1*$^{-/-}$ cells produced more infectious MLV/p6 viral particles than wt cells, whereas the two cells released almost the same amount of MLV (Fig. 5*E*). Therefore, it is likely that TBK1 aligned with VPS37C to affect only PTAP-dependent retroviral budding. This notion was further supported by the budding kinetics of EIAV virus-like particles. When the YPDL motif in EIAV Gag is replaced by PTAP (EIAV/PTAP), the derived virus-like particles released more efficiently in *Tbk1*$^{-/-}$ than in wt MEFs, whereas EIAV/PPPY budded at almost the same rate in the two cell types (Supplemental Fig. 4). Therefore, these results strongly implicated that TBK1 might specifically inhibit the release of PTAP-dependent retrovirus, and this inhibition was independent of its fundamental role in IFN-I induction.

IKK-i and TBK1 share 61% sequence identity and overlapped role in NF-κB activation and IFN-I production (43). Surprisingly, IKK-i also associated with ESCRT-I complex as revealed by coelution with TSG101 in the size exclusion chromatography (Fig. 6*A*). However, IKK-i did not contact VPS37C in coimmunoprecipitation experiments (Fig. 6*B*), and such a physical separation would suggest that IKK-i might not be essential for PTAP-dependent retroviral budding mediated by VPS37C. Agreeing with this prediction, lack of IKK-i did not affect MLV/p6 virus release, for MLV/p6 released as efficiently from *Ikk-i*$^{-/-}$ as from *wt* MEF cells (Fig. 6*C*). These and abovementioned results further implied the specific role for TBK1, but not IKK-i to regulate PTAP-dependent retrovirus budding.

The presence of TBK1 apparently controlled retroviral budding, but not other steps of the MLV/p6 life cycle. This could be demonstrated by the similar replication efficiency of MLV/p6 genome in either wt or *Tbk1*$^{-/-}$ MEFs along the time course examined (Supplemental Fig. 5*A*), with almost identical reverse transcription (minus strand strong stop DNA reaction), viral DNA synthesis (plus strand DNA reaction), and nuclear entry (MLV LTR–LTR junction reaction), as assessed by specific PCR detection (28). Neither did TBK1 affect ubiquitinylation of Gag, a modification required for MVB entry step in retroviral budding process (6), because Gag ubiquitinylation remained the same in wt or *Tbk1*$^{-/-}$ MEFs after MLV/p6 infection (Supplemental Fig. 5*B*). Furthermore, MLV/p6 virus particles produced by wt or *Tbk1*$^{-/-}$ MEFs were indistinguishable in their typical mature morphology (round, condensed concentric cores), as depicted by transmission

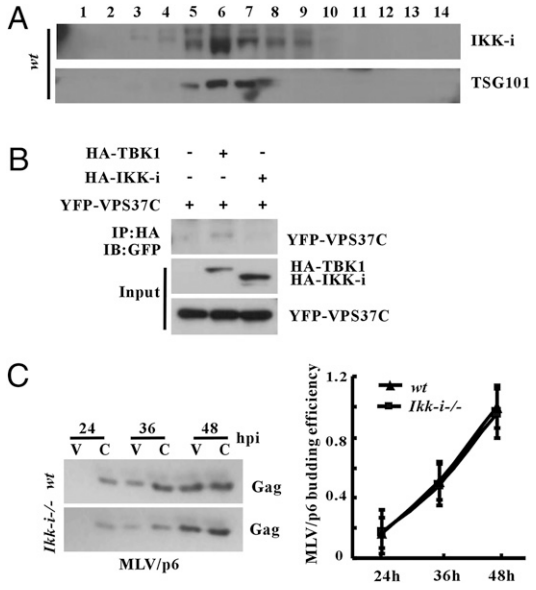

FIGURE 6. IKK-i is dispensable for MLV/p6 budding. *A*, Endogenous IKK-i coeluted with the ESCRT-I complex. Cell lysates of *wt* MEFs were fractionated as in Fig. 2*B*, and TCA-precipitated proteins were immunoblotted for IKK-i and TSG101. *B*, IKK-i did not interact with VPS37C. HEK293T cells were cotransfected with pEYFP-VPS37C and pEBB-HA-TBK1 or pEBB-HA-IKK-i, respectively. Coimmunoprecipitation was performed analogously as in Fig. 1*A* (*top panel*). The input of YFP-VPS37C, HA-TBK1, and HA-IKK-i was also shown (*bottom panels*). Data were representative of two independent experiments (*A*, *B*). *C*, IKK-i was not required for MLV/p6 budding. Budding efficiency was measured similarly as in Fig. 5, except that *Ikk-i*$^{-/-}$ MEFs were used. Data were the average of three independent experiments (mean ± SD).

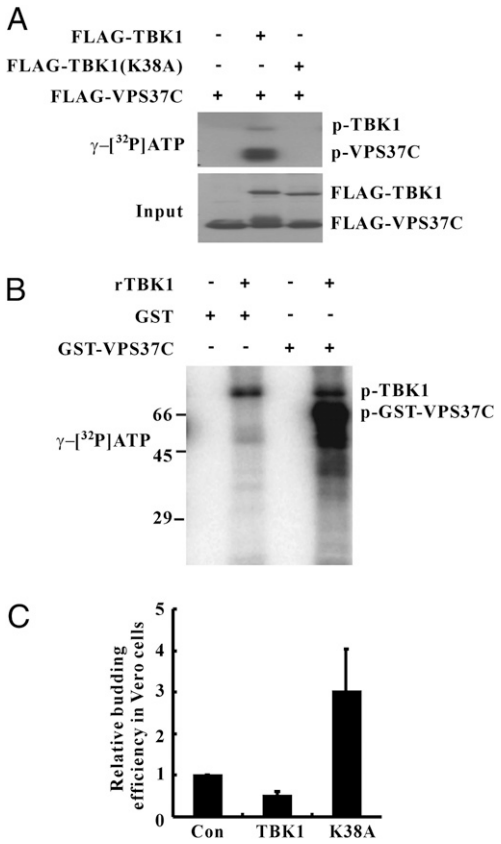

FIGURE 7. TBK1 dampens viral budding possibly by phosphorylating VPS37C. *A*, TBK1 phosphorylated VPS37C. Falg-tagged VPS37C, TBK1, or TBK1(K38A) was each immunoabsorbed to M2 agarose beads after transiently transfecting pCMV-Flag-VPS37C, pCMV-Flag-TBK1, or pCMV-Flag-TBK1(K38A) in 293T cells separately. Kinase assays were performed by mixing up bead-bound VPS37C and TBK1 or TBK1-K38A in the presence of γ-[^{32}P]ATP (*top panel*). Protein input levels were verified by immunoblotting (*bottom panel*). *B*, Recombinant TBK1 phosphorylated GST-VPS37C. In vitro kinase assays were performed by mixing recombinant GST or GST-VPS37C with recombinant human TBK1 in the presence of γ-[^{32}P]ATP. Phosphorylated proteins were separated by SDS-PAGE and scanned with a PhosphorImager. Data were representative of three independent experiments (*A*, *B*). *C*, Overexpressed TBK1(K38A) could increase HIV-1 pseudovirus budding. HIV-1 pseudovirus budding was assessed in Vero cells in the presence of cotransfected pECFP-TBK1 or pECFP-TBK1 (K38A), as in Fig. 4*A*. Data were average of six independent experiments (mean ± SD).

electron microscopy (Supplemental Fig. 5*C*). These results therefore clarified that TBK1 modulated PTAP-dependent MLV/p6 budding without affecting its genome replication, Gag ubiquitinylation, or assembly process.

TBK1 may regulate PTAP-dependent viral budding via phosphorylation of VPS37C

As TBK1 functions mainly as a Ser/Thr kinase, we set out to test whether TBK1 might regulate viral budding through phosphorylation of VPS37C. FLAG-tagged VPS37C and TBK1 were transiently expressed in 293T separately and immunoabsorbed individually on affinity beads. In vitro kinase assays by mixing up TBK1 and VPS37C beads showed that VPS37C was phosphorylated by wt, but not K38A mutant of TBK1 (Fig. 7*A*). To exclude the possibility that other kinase(s) might associate with immunoabsorbed TBK1, we then performed in vitro kinase assays using recombinant GST-VPS37C and recombinant TBK1, and the results showed TBK1 caused specific and significant phosphorylation of GST-VPS37C (Fig. 7*B*). In HIV-1 budding assay, whereas overexpressed TBK1 dampened viral release, kinase-inactive mutant TBK1-K38A enhanced budding from Vero cells (Fig. 7*C*). These results therefore indicated that phosphorylation of VPS37C by TBK1 correlated with inhibition of PTAP-dependent HIV-1 budding. However, the detailed mechanisms remain to be elucidated.

Discussion

TBK1 is a multifunctional kinase essential for NF-κB activation (16), type I IFN production (44), cell survival (45, 46), and recently documented restriction of bacterial proliferation in cytoplasm (20–22). We have identified that TBK1 may target and phosphorylate VPS37C, a structural component of ESCRT-I complex, and serve as a ratelimiting factor in the control of PTAP-dependent (HIV-1, MLV/p6, and EIAV/PTAP), but not PPPY-dependent (MLV, EIAV/PPPY) retrovirus budding, independent of its role in IFN-I signaling.

The association of TBK1 with the protein cargo system, which is often hijacked by the enveloped viruses for viral release, is quite intriguing. On the one hand, TBK1 did not affect the general structure or function of MVB; rather, it affects the specific facet of ESCRT-I by controlling of PTAP-dependent progeny retrovirus egress. This resembles the role of TBK1 in control of *Salmonella* replication by maintaining the integrity of pathogen-containing MVB without affecting its general function (20). On the other hand, although rather speculative, TBK1–VPS37C interaction may coevolve with the PTAP-dependent viruses to keep the virus infection and spread in check. Such a mechanism may become critical when host cells fail to produce sufficient IFN-I response to the invaded viruses.

Besides its canonical role of IFN-I signaling in innate immune responses, it becomes clear that TBK1 may contribute to the intrinsic host defense (intrinsic immunity) against pathogen infection. In *Salmonella* infection, TBK1 tightly regulates the level of aquaporin-1 protein (21), and maintains the integrity of the pathogen-containing vacuoles in fibroblast cytosol to control bacterial replication independent of its role in IFN-I induction (20). Our finding that TBK1 controls the speed of viral budding through direct interaction with ESCRT-I complex has also defined yet another intrinsic defense mechanism by TBK1 independent of IFN-I. Thus, in addition to its fundamental role in antiviral IFN-I production, TBK1 kinase activity may also engage in other critical cellular defense against pathogen infection, such as keeping pathogen-processing organelles in shape to control bacteria replication, and controlling the speed of PTAP-dependent viral release through ESCRT system.

The specificity of TBK1 in controlling PTAP-dependent retrovirus budding may be mediated by the specific intermolecular interaction with VPS37C, for the latter has been previously confirmed in the regulation of the PTAP-dependent virus release (7). TSG101 is also reported to play a central role in facilitating PTAP-dependent virus budding (37, 47, 48). However, we cannot observe the interaction between TBK1 and TSG101 in coimmunoprecipitation experiments (data not shown). Moreover, specific TBK1–VPS37C interaction within ESCRT-I complex may be of physiological significance, considering the facts that ESCRT-I complex is not only heterogeneous in composition, with four (9) VPS37 (VPS37A-D) and two (10) MVB12 (MVB12A and MVB12B) paralogs, but also distinctive in functions, as VPS37B and VPS37C function in HIV-1 budding (7, 9), whereas VPS37A mediates downregulation of receptors (49). It would be interesting to determine how TBK1–VPS37C interaction involves in only a specific facet of MVB function.

Phosphorylation of ESCRT-I components apparently involves in regulation of HIV-1 infection. For example, human MVB12A/B have been shown to possess a basal level of phosphorylation, and loss of phosphorylation by mutagenesis can partially alleviate the inhibitory effect of MVB12 on HIV-1 infectivity (10). We have been able to prove in this work that phosphorylation levels of VPS37C can be modulated by TBK1, which may contribute to the PTAP-dependent viral budding. More interestingly, retrovirus infection does not apparently activate TBK1 kinase activity in cytosol, if using IFN-I production as an indication. One reasonable explanation would be that retroviral infection may activate ESCRT-I–associated TBK1, whereas TBK1 recruited to the canonical IFN-I signaling machinery, probably in the endosome–mitochondria membrane system, remains inactivated. It is yet unclear whether any upstream pattern recognition receptor contributes to ESCRT-I–specific TBK1 activation upon virus budding. We are now in the process of comparing the TBK1 activities in ESCRT-I cargo system and endosome–mitochondria membrane system. Moreover, unlike the case of MVB12A, site-directed mutagenesis of VPS37C (36 Ser/Thr residues in all) individually or combinatorially fails to determine the critical site(s) that affects its phosphorylation or PTAP-dependent retrovirus release (data not shown). One possibility would be that appropriate phosphorylated VPS37C is required for the assembly of budding-competent ESCRT-I (considering that VPS37C is constitutively phosphorylated), and such a mutant is prohibited from ESCRT-I complex. It remains to be determined whether there is other TBK1 substrate(s) that is directly involved in budding process. Preliminary analysis has shown that TBK1-VPS37C interaction may help diverting virus to bud inward to MVBs instead of outward through cell membrane, for that more MLV/p6 virions within MVB have been observed in wt than in *Tbk1*$^{-/-}$ MEFs (Q. Da and H. Tang, unpublished data).

Acknowledgments

We thank Dr. Lishan Su (University of North Carolina), Dr. Andrea K. Perry (University of California, Los Angeles), and Dr. Yangxin Fu (University of Chicago) for critical reading and stimulating suggestions. We thank Drs. Tom Maniatis (Harvard University), Paul D. Bieniasz (Aaron Diamond AIDS Research Center), Alan Rein (National Cancer Institute), Binghong Shu (Wuhan University), Jianhua Zhou (Harbin Veterinary Research Institute), and Liguo Zhang (Institute of Biophysics, Chinese Academy of Sciences) for kindly providing various plasmids, reagents, and Abs. We also thank Drs. Jiaxin Liu (Wuhan Institute of Virology, Chinese Academy of Sciences), Shaobo Mo (Center for Analysis and Testing of Wuhan University), and Lei Sun (Institute of Biophysics, Chinese Academy of Sciences) for technical assistance in TEM imaging and analysis.

Disclosures

The authors have no financial conflicts of interest.

References

1. Hurley, J. H., and S. D. Emr. 2006. The ESCRT complexes: structure and mechanism of a membrane-trafficking network. *Annu. Rev. Biophys. Biomol. Struct.* 35: 277–298.
2. Williams, R. L., and S. Urbé. 2007. The emerging shape of the ESCRT machinery. *Nat. Rev. Mol. Cell Biol.* 8: 355–368.
3. Göttlinger, H. G. 2001. The HIV-1 assembly machine. *AIDS* 15(Suppl. 5): S13–S20.
4. Morita, E., and W. I. Sundquist. 2004. Retrovirus budding. *Annu. Rev. Cell Dev. Biol.* 20: 395–425.
5. Wills, J. W., and R. C. Craven. 1991. Form, function, and use of retroviral gag proteins. *AIDS* 5: 639–654.
6. Martin-Serrano, J. 2007. The role of ubiquitin in retroviral egress. *Traffic* 8: 1297–1303.
7. Eastman, S. W., J. Martin-Serrano, W. Chung, T. Zang, and P. D. Bieniasz. 2005. Identification of human VPS37C, a component of endosomal sorting complex required for transport-I important for viral budding. *J. Biol. Chem.* 280: 628–636.
8. Demirov, D. G., A. Ono, J. M. Orenstein, and E. O. Freed. 2002. Overexpression of the N-terminal domain of TSG101 inhibits HIV-1 budding by blocking late domain function. *Proc. Natl. Acad. Sci. USA* 99: 955–960.
9. Stuchell, M. D., J. E. Garrus, B. Müller, K. M. Stray, S. Ghaffarian, R. McKinnon, H. G. Kräusslich, S. G. Morham, and W. I. Sundquist. 2004. The human endosomal sorting complex required for transport (ESCRT-I) and its role in HIV-1 budding. *J. Biol. Chem.* 279: 36059–36071.
10. Morita, E., V. Sandrin, S. L. Alam, D. M. Eckert, S. P. Gygi, and W. I. Sundquist. 2007. Identification of human MVB12 proteins as ESCRT-I subunits that function in HIV budding. *Cell Host Microbe* 2: 41–53.
11. Bieniasz, P. D. 2006. Late budding domains and host proteins in enveloped virus release. *Virology* 344: 55–63.
12. Freed, E. O. 2002. Viral late domains. *J. Virol.* 76: 4679–4687.
13. Takeuchi, O., and S. Akira. 2009. Innate immunity to virus infection. *Immunol. Rev.* 227: 75–86.
14. Malmgaard, L. 2004. Induction and regulation of IFNs during viral infections. *J. Interferon Cytokine Res.* 24: 439–454.
15. Perry, A. K., G. Chen, D. Zheng, H. Tang, and G. Cheng. 2005. The host type I interferon response to viral and bacterial infections. *Cell Res.* 15: 407–422.
16. Pomerantz, J. L., and D. Baltimore. 1999. NF-kappaB activation by a signaling complex containing TRAF2, TANK and TBK1, a novel IKK-related kinase. *EMBO J.* 18: 6694–6704.
17. Kishore, N., Q. K. Huynh, S. Mathialagan, T. Hall, S. Rouw, D. Creely, G. Lange, J. Caroll, B. Reitz, A. Donnelly, et al. 2002. IKK-i and TBK-1 are enzymatically distinct from the homologous enzyme IKK-2: comparative analysis of recombinant human IKK-i, TBK-1, and IKK-2. *J. Biol. Chem.* 277: 13840–13847.
18. Soulat, D., T. Bürckstümmer, S. Westermayer, A. Goncalves, A. Bauch, A. Stefanovic, O. Hantschel, K. L. Bennett, T. Decker, and G. Superti-Furga. 2008. The DEAD-box helicase DDX3X is a critical component of the TANK-binding kinase 1-dependent innate immune response. *EMBO J.* 27: 2135–2146.
19. Clark, K., L. Plater, M. Peggie, and P. Cohen. 2009. Use of the pharmacological inhibitor BX795 to study the regulation and physiological roles of TBK1 and IkappaB kinase epsilon: a distinct upstream kinase mediates Ser-172 phosphorylation and activation. *J. Biol. Chem.* 284: 14136–14146.
20. Radtke, A. L., L. M. Delbridge, S. Balachandran, G. N. Barber, and M. X. O'Riordan. 2007. TBK1 protects vacuolar integrity during intracellular bacterial infection. *PLoS Pathog.* 3: e29.
21. Radtke, A. L., and M. X. O'Riordan. 2008. Homeostatic maintenance of pathogen-containing vacuoles requires TBK1-dependent regulation of aquaporin-1. *Cell. Microbiol.* 10: 2197–2207.
22. Thurston, T. L., G. Ryzhakov, S. Bloor, N. von Muhlinen, and F. Randow. 2009. The TBK1 adaptor and autophagy receptor NDP52 restricts the proliferation of ubiquitin-coated bacteria. *Nat. Immunol.* 10: 1215–1221.
23. Yuan, B., S. Campbell, E. Bacharach, A. Rein, and S. P. Goff. 2000. Infectivity of Moloney murine leukemia virus defective in late assembly events is restored by late assembly domains of other retroviruses. *J. Virol.* 74: 7250–7260.
24. Adachi, A., H. E. Gendelman, S. Koenig, T. Folks, R. Willey, A. Rabson, and M. A. Martin. 1986. Production of acquired immunodeficiency syndrome-associated retrovirus in human and nonhuman cells transfected with an infectious molecular clone. *J. Virol.* 59: 284–291.
25. Koyanagi, Y., S. Miles, R. T. Mitsuyasu, J. E. Merrill, H. V. Vinters, and I. S. Chen. 1987. Dual infection of the central nervous system by AIDS viruses with distinct cellular tropisms. *Science* 236: 819–822.
26. Endres, M. J., S. Jaffer, B. Haggarty, J. D. Turner, B. J. Doranz, P. J. O'Brien, D. L. Kolson, and J. A. Hoxie. 1997. Targeting of HIV- and SIV-infected cells by CD4-chemokine receptor pseudotypes. *Science* 278: 1462–1464.
27. Gottwein, E., J. Bodem, B. Müller, A. Schmechel, H. Zentgraf, and H. G. Kräusslich. 2003. The Mason-Pfizer monkey virus PPPY and PSAP motifs both contribute to virus release. *J. Virol.* 77: 9474–9485.
28. Gao, G. X., and S. P. Goff. 1999. Somatic cell mutants resistant to retrovirus replication: intracellular blocks during the early stages of infection. *Mol. Biol. Cell* 10: 1705–1717.
29. Joshi, A., U. Munshi, S. D. Ablan, K. Nagashima, and E. O. Freed. 2008. Functional replacement of a retroviral late domain by ubiquitin fusion. *Traffic* 9: 1972–1983.
30. Zheng, D., G. Chen, B. Guo, G. Cheng, and H. Tang. 2008. PLP2, a potent deubiquitinase from murine hepatitis virus, strongly inhibits cellular type I interferon production. *Cell Res.* 18: 1105–1113.
31. Alwan, H. A. J., and J. E. M. van Leeuwen. 2007. UBPY-mediated epidermal growth factor receptor (EGFR) de-ubiquitination promotes EGFR degradation. *J. Biol. Chem.* 282: 1658–1669.
32. Razi, M., and C. E. Futter. 2006. Distinct roles for Tsg101 and Hrs in multivesicular body formation and inward vesiculation. *Mol. Biol. Cell* 17: 3469–3483.
33. Melchjorsen, J., S. B. Jensen, L. Malmgaard, S. B. Rasmussen, F. Weber, A. G. Bowie, S. Matikainen, and S. R. Paludan. 2005. Activation of innate defense against a paramyxovirus is mediated by RIG-I and TLR7 and TLR8 in a cell-type-specific manner. *J. Virol.* 79: 12944–12951.
34. tenOever, B. R., S. Sharma, W. Zou, Q. Sun, N. Grandvaux, I. Julkunen, H. Hemmi, M. Yamamoto, S. Akira, W. C. Yeh, et al. 2004. Activation of TBK1 and IKKvarepsilon kinases by vesicular stomatitis virus infection and the role of viral ribonucleoprotein in the development of interferon antiviral immunity. *J. Virol.* 78: 10636–10649.
35. Berger, B., D. B. Wilson, E. Wolf, T. Tonchev, M. Milla, and P. S. Kim. 1995. Predicting coiled coils by use of pairwise residue correlations. *Proc. Natl. Acad. Sci. USA* 92: 8259–8263.
36. Winter, V., and M. T. Hauser. 2006. Exploring the ESCRTing machinery in eukaryotes. *Trends Plant Sci.* 11: 115–123.
37. Garrus, J. E., U. K. von Schwedler, O. W. Pornillos, S. G. Morham, K. H. Zavitz, H. E. Wang, D. A. Wettstein, K. M. Stray, M. Côté, R. L. Rich, et al. 2001. Tsg101 and the vacuolar protein sorting pathway are essential for HIV-1 budding. *Cell* 107: 55–65.
38. Desmyter, J., J. L. Melnick, and W. E. Rawls. 1968. Defectiveness of interferon production and of rubella virus interference in a line of African green monkey kidney cells (Vero). *J. Virol.* 2: 955–961.
39. Platt, E. J., K. Wehrly, S. E. Kuhmann, B. Chesebro, and D. Kabat. 1998. Effects of CCR5 and CD4 cell surface concentrations on infections by macrophagetropic isolates of human immunodeficiency virus type 1. *J. Virol.* 72: 2855–2864.
40. Wei, X., J. M. Decker, H. Liu, Z. Zhang, R. B. Arani, J. M. Kilby, M. S. Saag, X. Wu, G. M. Shaw, and J. C. Kappes. 2002. Emergence of resistant human immunodeficiency virus type 1 in patients receiving fusion inhibitor (T-20) monotherapy. *Antimicrob. Agents Chemother.* 46: 1896–1905.
41. Feng, Y., C. C. Broder, P. E. Kennedy, and E. A. Berger. 1996. HIV-1 entry cofactor: functional cDNA cloning of a seven-transmembrane, G protein-coupled receptor. *Science* 272: 872–877.
42. Simmons, G., D. Wilkinson, J. D. Reeves, M. T. Dittmar, S. Beddows, J. Weber, G. Carnegie, U. Desselberger, P. W. Gray, R. A. Weiss, and P. R. Clapham. 1996. Primary, syncytium-inducing human immunodeficiency virus type 1 isolates are dual-tropic and most can use either Lestr or CCR5 as coreceptors for virus entry. *J. Virol.* 70: 8355–8360.
43. Clément, J. F., S. Meloche, and M. J. Servant. 2008. The IKK-related kinases: from innate immunity to oncogenesis. *Cell Res.* 18: 889–899.
44. Häcker, H., and M. Karin. 2006. Regulation and function of IKK and IKK-related kinases. *Sci. STKE* 2006: re13.
45. Bonnard, M., C. Mirtsos, S. Suzuki, K. Graham, J. Huang, M. Ng, A. Itié, A. Wakeham, A. Shahinian, W. J. Henzel, et al. 2000. Deficiency of T2K leads to apoptotic liver degeneration and impaired NF-kappaB-dependent gene transcription. *EMBO J.* 19: 4976–4985.
46. Chien, Y., S. Kim, R. Bumeister, Y. M. Loo, S. W. Kwon, C. L. Johnson, M. G. Balakireva, Y. Romeo, L. Kopelovich, M. Gale, Jr. et al. 2006. RalB GTPase-mediated activation of the IkappaB family kinase TBK1 couples innate immune signaling to tumor cell survival. *Cell* 127: 157–170.
47. Martin-Serrano, J., T. Zang, and P. D. Bieniasz. 2001. HIV-1 and Ebola virus encode small peptide motifs that recruit Tsg101 to sites of particle assembly to facilitate egress. *Nat. Med.* 7: 1313–1319.
48. VerPlank, L., F. Bouamr, T. J. LaGrassa, B. Agresta, A. Kikonyogo, J. Leis, and C. A. Carter. 2001. Tsg101, a homologue of ubiquitin-conjugating (E2) enzymes, binds the L domain in HIV type 1 Pr55(Gag). *Proc. Natl. Acad. Sci. USA* 98: 7724–7729.
49. Bache, K. G., T. Slagsvold, A. Cabezas, K. R. Rosendal, C. Raiborg, and H. Stenmark. 2004. The growth-regulatory protein HCRP1/hVps37A is a subunit of mammalian ESCRT-I and mediates receptor down-regulation. *Mol. Biol. Cell* 15: 4337–4346.